# Out-of-plane exchange bias in [Pt/Co]–IrMn bilayers sputtered on prepatterned nanostructures

A. Bollero, Vincent Baltz, B. Rodmacq, B. Dieny, S. Landis, J. Sort

# Out-of-plane exchange bias in [Pt/Co]–IrMn bilayers sputtered on prepatterned nanostructures

A. Bollero,[a] V. Baltz,[b] B. Rodmacq, and B. Dieny
*SPINTEC (URA 2512 CNRS/CEA), CEA-Grenoble, 17 Av. Martyrs, 38054 Grenoble Cedex 9, France*

S. Landis
*LETI/D2NT, CEA Grenoble, 17 Av. Martyrs, 38054 Grenoble Cedex 9, France*

J. Sort
*Institució Catalana de Recerca i Estudis Avançats (ICREA), and Departament de Física, Facultat de Ciències, Universitat Autònoma de Barcelona, 08193 Bellaterra, Spain*

(Received 23 February 2006; accepted 17 August 2006; published online 9 October 2006)

Exchange bias effects along the out-of-plane direction have been investigated in arrays of 100 nm nanostructures prepared on top of prepatterned substrates, consisting of a ferromagnetic [Pt/Co] multilayer with out-of-plane anisotropy exchange coupled to an antiferromagnetic IrMn layer. A significant loop shift is observed in these nanostructures (dots and trenches). The relative evolutions of the bias fields with the IrMn thickness in the nanostructures and in the continuous film are ascribed to both the effects of the IrMn domain size and thermal activation. Lower coordinated spins in the trenches and at the dot edges are assumed to play a key role on the bias properties. A reduction of the blocking temperature is observed for both the dots and the trenches with respect to the continuous film. © *2006 American Institute of Physics*. [DOI: 10.1063/1.2359429]

Exchange bias (EB) refers to a shift of the hysteresis loop along the magnetic field axis by a quantity termed exchange bias field $H_E$. It typically results from the interfacial coupling between ferromagnetic (FM) and antiferromagnetic (AFM) layers. The loop shift is usually accompanied by an increase in the coercivity.[1] These systems have been extensively investigated due to their technological applications in magnetic sensors based on spin valves or magnetic tunnel junctions.[2,3] The increase of the data storage densities points to the necessity of a miniaturization of these devices. So far, most of the studies dealing with EB based structures of reduced lateral dimensions have been carried out on systems with in-plane magnetic anisotropy.[4] Sensors, such as read heads, with out-of-plane magnetic anisotropy would, however, be interesting in order to further increase the storage densities.[5] Although several studies have been published on the EB phenomenon induced along the out-of-plane direction in continuous films,[6–9] the effects of reduced lateral dimensions on the out-of-plane EB have been far less investigated. Moreover, they have often led to the conclusion of a nonsignificant bias energy for structures with a characteristic size below a few hundreds of nanometers.[10,11]

In this letter, the evolution of the out-of-plane EB phenomenon has been studied in nanostructured [Pt/Co]–IrMn systems in which the IrMn layer thickness and the number of Pt/Co repetitions were varied. Relatively large bias fields of tunable amplitude can be obtained in these nanostructures, when they are deposited onto prepatterned substrates. However, the blocking temperature in the nanostructures (dots and trenches) is lower than in the continuous film.

Si wafers were first patterned to form arrays of Si square dots, with lateral sizes of 100 nm, height of 200 nm, and edge to edge spacing of 100 nm (see inset of Fig. 1). Two series of multilayers with compositions of $[\mathrm{Pt}(2\ \mathrm{nm})/\mathrm{Co}(0.6\ \mathrm{nm})]_3/\mathrm{IrMn}(t_{\mathrm{IrMn}})/\mathrm{Pt}(2\ \mathrm{nm})$ and $[\mathrm{Pt}(2\ \mathrm{nm})/\mathrm{Co}(0.6\ \mathrm{nm})]_n/\mathrm{IrMn}(5\ \mathrm{nm})/\mathrm{Pt}(2\ \mathrm{nm})$ (where IrMn stands for $Ir_{20}Mn_{80}$) were dc-magnetron sputtered on these naturally oxidized patterned wafers thereby coating the patterned (dots and trenches) and surrounding unpatterned (continuous) regions.[12] The IrMn thickness $t_{\mathrm{IrMn}}$, and the number of Pt/Co repetitions $n$ were varied from 5 to 19 nm and from 2 to 5, respectively. The layers were sputtered with a perpendicular-to-plane incidence and hence cover the top of the pillar (dots) and the inter dot regions (trenches). Previous magnetic force microscopy measurements have revealed that the magnetization of dots with dimensions comparable to ours can be up or down independently from the magnetization direction in the trenches.[12] This might be an indication of the dots and trenches being virtually magnetically decoupled. Cross-section transmission electron microscopy images of silicon lines (with a width of 100 nm and a height of 300 nm) coated with sputtered [Co/Pt] revealed the presence of granular material on the side wall of the lines.[12] However, this material seems to consist of disconnected grains which might favor the absence of direct coupling between the magnetic material at the top of the dots and in the trenches. To set EB, the samples were postannealed and field

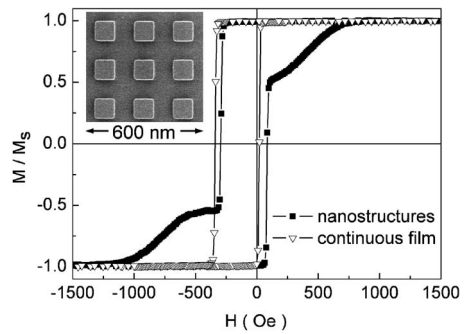


FIG. 1. Hysteresis loops of the continuous films and the nanostructures (dots and trenches) with composition of $[\mathrm{Pt}(2\ \mathrm{nm})/\mathrm{Co}(0.6\ \mathrm{nm})]_3/\mathrm{IrMn}(9\ \mathrm{nm})/\mathrm{Pt}(2\ \mathrm{nm})$. The inset shows a scanning electron microscopy image of the nanostructures.

[a]Electronic mail: alberto_bollero@yahoo.es
[b]Electronic mail: v-baltz@spintec.fr

 

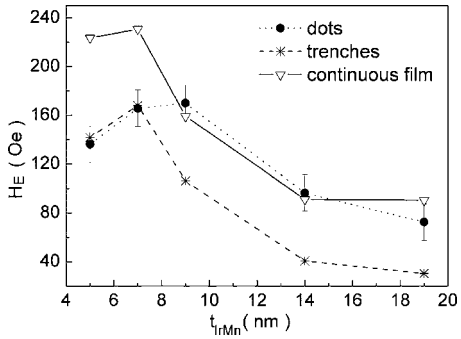


FIG. 2. Evolutions of the exchange bias field $H_E$ with the IrMn thickness $t_{IrMn}$ for $[Pt(2\ nm)/Co(0.6\ nm)]_3/IrMn(t_{IrMn})/Pt(2\ nm)$ stacks.

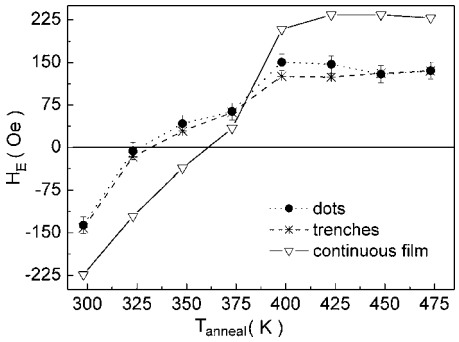


FIG. 3. Dependence of the exchange bias field $H_E$ on the annealing temperature $T_{anneal}$ for $[Pt(2\ nm)/Co(0.6\ nm)]_3/IrMn(5\ nm)/Pt(2\ nm)$ stacks.

cooled from $T=550$ K (above the blocking temperature of all systems) under a 2.4 kOe magnetic field, applied along the out-of-plane direction. Hysteresis loops were measured at room temperature, along the field cooling direction, using a polar Kerr effect setup. Either the continuous films or the nanostructures (dots and trenches at the same time) were probed by focusing the laser spot accordingly. The blocking temperature distributions in the dots, trenches, and continuous film were evaluated by field cooling the samples under a negative field from various temperatures ranging from 300 to 550 K, after the standard cooling procedure.[13]

Figure 1 shows typical hysteresis loops recorded on the nanostructured region and on the continuous film with composition of $[Pt(2\ nm)/Co(0.6\ nm)]_3/IrMn(9\ nm)/Pt(2\ nm)$. The continuous film displays the expected shifted square loop with a 100% remanence to saturation ratio.[9] For the nanostructures, two shifted loops can be clearly distinguished. As already observed[14] and owing to the deposition and measurement geometries, both the signals from the dots and that from the trenches can be differentiated. The sharp transitions, at relatively low fields, correspond to the magnetization reversal of the trenches, while the second ones, much broader and at higher fields, are ascribed to the magnetization reversal of the dots. The significant broadening of the transition observed for the dots has been previously reported and attributed to inhomogeneities among the dots which results in a switching field distribution.[10,12] It has to be noted that in both cases, the remanence to saturation ratio remains close to 1. Additional magnetic force microscopy images (not shown) allowed us to confirm that in the remanent state, the dots are in an out-of-plane single domain configuration.

As can be seen in Fig. 1, the coercive field of the dots (~600 Oe) is much larger than that of the trenches (~190 Oe) and continuous film (~180 Oe). This effect has been previously observed in patterned systems and has been attributed to the reduced amount of effective nucleation centers for the dots and to a possible change in the magnetization reversal mechanism in comparison with the continuous film.[10,14–16] In addition, the dot boundaries play a major role in pinning the magnetization and, in the patterned structures, the boundary constitutes a more significant part of the structure relative to the total volume and hence the coercivity concomitantly increases.

In comparison with earlier studies on out-of-plane EB nanostructures in the literature,[10,11] we observe a significant bias field for the dots of about 180 Oe (see Fig. 1), which corresponds to an exchange energy of around $4.5\times10^{-2}$ erg cm$^{-2}$. The achievement of large pinning energy at small lateral dimensions is a key issue for the downsizing of spin electronic devices.[1] The results obtained in this study are ascribed to the preparation technique, which relies on the use of prepatterned wafers thereby avoiding possible material degradation effects due to post-deposition etching in contrast to earlier studies.[12,16]

The understanding of the magnitudes of the bias fields in dots, trenches, and continuous film requires taking into account the role of AFM domains (whose size depends on the AFM thickness) along with thermal activation effects.[17]

The evolutions of the bias field $H_E$ as a function of the IrMn layer thickness $t_{IrMn}$ for the dots, the trenches, and the continuous films are shown in Fig. 2.

For the continuous films, above 5 nm of IrMn, the bias field decreases with increasing the IrMn layer thickness, as typically reported experimentally and explained theoretically.[1,18] It has actually been derived that the bias field is inversely proportional to the AFM domain size which itself increases with increasing the AFM layer thickness.[18]

Interestingly, the dots show a different behavior, notably for thin IrMn layers. The bias field increases slightly between $t_{IrMn}=5$ and 9 nm and then decreases with increasing the IrMn layer thickness. It is also important to note that while for thin IrMn the bias field is smaller for the dots with respect to the continuous film, for thicker IrMn (above $t_{IrMn}=9$ nm) the evolutions of $H_E$ with $t_{IrMn}$ for the dots and for the continuous film match. Such an observation results from the interplay between constraints in the AFM domain formation and thermal activation effects.[17] Given the inverse proportionality between the bias field and the IrMn domain size, it has been previously discussed[17] that the constraints on the IrMn domain size (which, in continuous film, range from ~150 to ~600 nm for $t_{IrMn}$ ranging from 5 to 19 nm) physically imposed by the reduced lateral dimensions of the dots (100 nm) favor an enhancement of the bias field for the dots with respect to the continuous films. Moreover, it has been suggested that the reduced coordination of the spins located at the edges of the dots makes them certainly more prone to thermal activation which, in turn, supports a reduction of the bias field in the dots.[17]

Using a standard cooling procedure, we were able to justify that in systems with out-of-plane anisotropy, the dots are more subject to thermal activation effects than the continuous films. Figure 3 shows the evolutions of the exchange bias field $H_E$ with the annealing temperature $T_{anneal}$ from which the samples have been field cooled in a negative field.[13] This allows estimating the blocking temperature distribution which stems from local variations in interface roughness or AFM crystallite sizes. As shown in Fig. 3, the

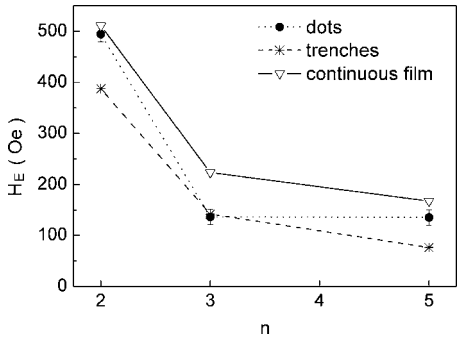


FIG. 4. Evolutions of the exchange bias field $H_E$ with the number of Pt/Co repeats $n$ for $[Pt(2\ nm)/Co(0.6\ nm)]_n/IrMn(5\ nm)/Pt(2\ nm)$ stacks.

magnitude of the bias field, measured at room temperature, decreases and changes sign as the annealing temperature is increased. The relative change in bias field is ascribed to the number of IrMn regions with local blocking temperatures lower than $T_{anneal}$ and which pinning direction was thus reversed during the second annealing procedure. $H_E$ vanishes at $T_{anneal} \sim 330$ K for the dots, whereas it vanishes at a higher annealing temperature ($\sim$365 K) for the continuous film. Additionally, the temperature at which the bias field levels off after field cooling in a negative field corresponds to the maximum local blocking temperature $T_B$ and seems to be also slightly smaller (by about 25 K) for the dots than for the continuous film. These results confirm that the exchange biased dots are more prone to thermal activation effects than the continuous films.

In Fig. 2 we observe that the bias field in the trenches decreases when the IrMn layer thickness is increased and is smaller than that in the continuous films over the whole range of IrMn layer thickness studied. Moreover, for thin IrMn layers, the magnitude of the bias field in the trenches is similar to that in the dots while, unexpectedly, for thicker IrMn, it becomes smaller in the trenches than in the dots.

Such behaviors can be ascribed to the presence of more weakly coordinated spins at the trenches, which seem to play a key role in the observed phenomenon. In the trenches, such spins with a lesser number of neighbors are located at the bottom of each dot pillar. These spins, in the trenches, would behave in a similar way to weakly coordinated spins located at the edges of the top of the dots. They are also expected to be very prone to thermal activation which results in an overall reduction of the bias field in the trenches with respect to the continuous film. Furthermore, in contrast to the dots, the interconnection existing between the trenches avoids the physical constraints imposed on the IrMn domain size originating from limitations in the lateral dimensions. As a result, the bias field decreases as the IrMn layer thickness increases, as it occurs for the continuous films due to the inverse relationship between the bias field and the AFM domain size, which is proportional to the IrMn thickness.

The evolution of the exchange bias field $H_E$ in the trenches with the annealing temperature $T_{anneal}$, shown in Fig. 3, is practically identical to that for the dots. Namely, the trenches with $t_{IrMn}=5$ nm also exhibit a blocking temperature lower than for the continuous film, which confirms the fact that they are more prone to thermal activation.

The matching between (i) the magnitude of the bias field for the trenches and the dots for thin IrMn ($t_{IrMn}<7$ nm, see Fig. 2) and (ii) the temperature evolutions of the bias fields for the dots and the trenches (see Fig. 3) are both the result of the more weakly coordinated spins located at the bottom of the dot pillars in the trenches and at the edges of the top of the dots. These spins are likely to favor an overall reduction of the bias field with respect to the continuous film.

Figure 4 shows the evolutions of the bias field $H_E$ with the number of Pt/Co repetitions $n$ (i.e., with the FM layer thickness) for the dots, the trenches, and the continuous films. In all cases, $H_E$ is reduced when $n$ is increased, as typically observed in out-of-plane EB continuous bilayers.[9] The scaling of this trend had not been reported so far for trenches or reduced dimension bilayers with out-of-plane anisotropy. Such evolutions confirm the interfacial nature of the hysteresis loop shift resulting from FM-AFM coupling in dots, trenches, and continuous films.

In conclusion, we have shown that it is possible to induce a significant loop shift, in out-of-plane exchange biased [Pt/Co]/IrMn dots with lateral sizes of 100 nm. We ascribe this contrasted behavior to the use of a prepatterning method which avoids postdeposition degradation of the material associated with the process of nanopatterning. The relative evolutions of the bias fields with the IrMn thickness have allowed us to point out the key role of the more weakly coordinated spins at the edges of the dots and at the bottom of the dot pillars in the trenches.

The authors would like to thank M. Jamet. This work was supported by the European Community through the NEXBIAS Grant No. HPRN-CT-2002-00296.

[1]For recent reviews, see J. Nogués and I. K. Schuller, J. Magn. Magn. Mater. **192**, 203 (1999); A. E. Berkowitz and K. Takano, *ibid.* **200**, 552 (1999); R. L. Stamps, J. Phys. D **33**, R247 (2000); M. Kiwi, J. Magn. Magn. Mater. **234**, 584 (2001).
[2]B. Dieny, V. S. Speriosu, S. S. P. Parkin, B. A. Gurney, D. R. Wilhoit, and D. Mauri, Phys. Rev. B **43**, 1297 (1991).
[3]S. Tehrani, J. M. Slaughter, M. Deherrera, B. N. Engel, N. D. Rizzo, J. Slater, M. Durlam, R. W. Dave, J. Janesky, B. Butcher, K. Smith, and G. Grynkewich, Proc. IEEE **91**, 703 (2003).
[4]J. Nogués, J. Sort, V. Langlais, S. Suriñach, J. S. Muñoz, and M. D. Baró, Phys. Rep. **422**, 62 (2005).
[5]A. Moser, K. Takano, D. T. Margulies, M. Albrecht, Y. Sonobe, Y. Ikeda, S. Sun, and E. E. Fullerton, J. Phys. D **35**, 157 (2002).
[6]B. Kagerer, Ch. Binek, and W. Kleemann, J. Magn. Magn. Mater. **217**, 139 (2000).
[7]S. Maat, K. Takano, S. S. P. Parkin, and E. E. Fullerton, Phys. Rev. Lett. **87**, 087202 (2001).
[8]F. Garcia, G. Casali, S. Auffret, B. Rodmacq, and B. Dieny, J. Appl. Phys. **91**, 6905 (2002).
[9]J. Sort, V. Baltz, F. Garcia, B. Rodmacq, and B. Dieny, Phys. Rev. B **71**, 054411 (2005).
[10]J. Sort, B. Dieny, M. Fraune, C. Koenig, F. Lunnebach, B. Beschoten, and G. Güntherodt, Appl. Phys. Lett. **84**, 3696 (2004).
[11]J. L. Menéndez, D. Ravelosona, and C. Chappert, J. Appl. Phys. **95**, 6726 (2004).
[12]S. Landis, B. Rodmacq, and B. Dieny, Phys. Rev. B **62**, 12271 (2000); S. Landis, thesis, Université Joseph Fourier de Grenoble, 2001.
[13]S. Soeya, S. Nakamura, T. Imagawa, and S. Narishige, J. Appl. Phys. **77**, 5838 (1995); S. Soeya, T. Himagawa, K. Mitsuoka, and S. Narishige, *ibid.* **76**, 5356 (1994).
[14]M. Albrecht, G. Hu, A. Moser, O. Hellwig, and B. D. Terris, J. Appl. Phys. **97**, 103910 (2005).
[15]J. Moritz, B. Dieny, J. P. Nozières, Y. Pennec, J. Camarero, and S. Pizzini, Phys. Rev. B **71**, 100402(R) (2005).
[16]J. I. Martin, J. Nogués, K. Liu, J. L. Vicent, and I. K. Schuller, J. Magn. Magn. Mater. **256**, 449 (2003).
[17]V. Baltz, J. Sort, S. Landis, B. Rodmacq, and B. Dieny, Phys. Rev. Lett. **94**, 117201 (2005).
[18]A. P. Malozemoff, Phys. Rev. B **35**, 3679 (1987); **37**, 7673 (1988).